ADVANCED FUNCTIONAL MATERIALS
www.afm-journal.de

Improving the ON/OFF Ratio and Reversibility of Recording by Rational Structural Arrangement of Donor–Acceptor Molecules

By *Ying Ma, Xingbo Cao, Guo Li, Yongqiang Wen,* Ye Yang, Jingxia Wang, Shixuan Du, Lianming Yang, Hongjun Gao,* and *Yanlin Song**

Organic molecules with donor–acceptor (D–A) structure are an important type of material for nanoelectronics and molecular electronics. The influence of the electron donor and acceptor units on the electrical function of materials is a worthy topic for the development of high-performance data storage. In this work, the effect of different D–A structures (namely D–л–A–л–D and A–л–D–л–A) on the electronic switching properties of triphenylamine-based molecules is investigated. Devices based on D–л–A–л–D molecules exhibit excellent write–read–erase characteristics with a high ON/OFF ratio of up to 10^6, while that based on A–л–D–л–A molecules exhibit irreversible switching behavior with an ON/OFF ratio of about (3.2×10^1)–(1×10^3). Moreover, long retention time of the high conductance state and low threshold voltage are observed for the D–A switching materials. Accordingly, stable and reliable nanoscale data storage is achieved on the thin films of the D–A molecules by scanning tunneling microscopy. The influence of the arrangement of the D and A within the molecular backbone disclosed in this study will be of significance for improving the electronic switching properties (ON/OFF current ratio and reversibility) of new molecular systems, so as to achieve more efficient data storage through appropriate design strategies.

1. Introduction

Organic materials exhibiting bistable conductance switching have been extensively investigated due to their potential applications for data storage.[1,2] A wide range of materials, including conjugated polymers,[3–8] oligomers,[9,10] small organic molecules,[11–20] and blends of nanoparticles in an organic host[21–23] have been reported for electrical switching and memory effects. In particular, organic donor–acceptor (D–A) molecules, due to their ability to exhibit electrical bistability and versatility in molecular design, have received considerable attention.[24–26] Furthermore, large-scale and smoother thin films can be easily fabricated by vacuum evaporation and deposition.[26,27] Up to now, extensive investigations have been made to develop D–A switching materials with excellent properties to meet the requirements of high-density data storage. However, the research has been mainly focused on the exploration of different D–A molecules with better electrical properties for data storage. The role of the donor and acceptor in the D–A structure, especially the influence of the arrangement of the donor and acceptor within the molecular backbone on the electronic switching properties, has rarely been systematically studied. This situation calls for a deeper understanding of the structure–property relationship to help the design of new D–A molecules.

In this work, we designed and synthesized a new series of D–A molecules with similar electron donor and acceptor units. Based on different arrangements of the donor and acceptor units, the D–A molecules were designed as two structural types, namely D–л–A–л–D and A–л–D–л–A. Here, triphenylamine (TPA) units are selected as the electron donor because of their strong ability for electron-donating. In addition, triphenylamine units possess excellent hole-transporting abilities, which can be expected to modify the electrical conductivity of the material effectively.[28–30] The acceptor moieties mainly contain cyanide-substituted vinyl groups with neighboring benzene rings. The study showed that the arrangement of the donor and acceptor within the molecular backbone plays a key role for the electrical

[*] Dr. Y. Wen, Prof. Y. Song, Dr. Y. Ma, Dr. X. Cao, Dr. J. Wang, Prof. L. Yang
Beijing National Laboratory for Molecular Sciences (BNLMS)
Key Laboratory of Organic Solids
Laboratory of New Materials
Institute of Chemistry
Chinese Academy of Sciences
Beijing, 100190 (P. R. China)
E-mail: wyq_wen@iccas.ac.cn; ylsong@iccas.ac.cn
Dr. Y. Ma, Dr. X. Cao
Graduate School of Chinese Academy of Science
Beijing, 100049 (P. R. China)
Dr. G. Li, Dr. Y. Yang, Dr. S. Du, Prof. H. Gao
Nanoscale Physics and Device Laboratory
Institute of Physics
Chinese Academy of Sciences
Beijing, 100190 (P. R. China)

DOI: 10.1002/adfm.200901692

memory behavior of the devices. The devices based on the D–л–A–л–D molecule exhibited excellent write–read–erase characteristics with a high ON/OFF ratio of up to 10^6, while that based on the A–л–D–л–A molecule exhibited irreversible switching behavior and a relatively low ON/OFF ratio ((3.2×10^1)–(1×10^3)). This research was meaningful for understanding the effect of the different D–A arrangements and effectively regulating the electronic switching properties (ON/OFF current ratio, reversibility, etc.) through rational organization of the donor and acceptor. Accordingly, stable and reliable nanoscale data storage was achieved on the thin films of the D–A molecules by scanning tunneling microscopy (STM). This work takes an important step towards rational design of new organic D–A molecules with suitable structures for high-performance data storage.

2. Results and Discussion

2.1. Material Properties

The D–A molecules investigated in this work are bis{4-[4-[di(*p*-tolyl)amino]phenyl]phenyl}fumaronitrile (TPDBCN), *N,N′*-bis[4-(1,1-dicyanovinyl)phenyl]-*N,N′*-diphenylbenzidine (TPDYCN1), and *N,N′*-bis[4-(1,1-dicyanovinyl)phenyl]-*N,N′*-bis(4-methoxyphenyl)benzidine (TPDYCN2). In addition, a D–л–D structural molecule (*N,N,N′,N′*-tetra(4-methylphenyl)-(1,1′-biphenyl)-4,4′-diamine (TTB)) was also studied to understand the electrical switching behavior of the D–A molecules. The molecular structures of the materials are shown in Figure 1.

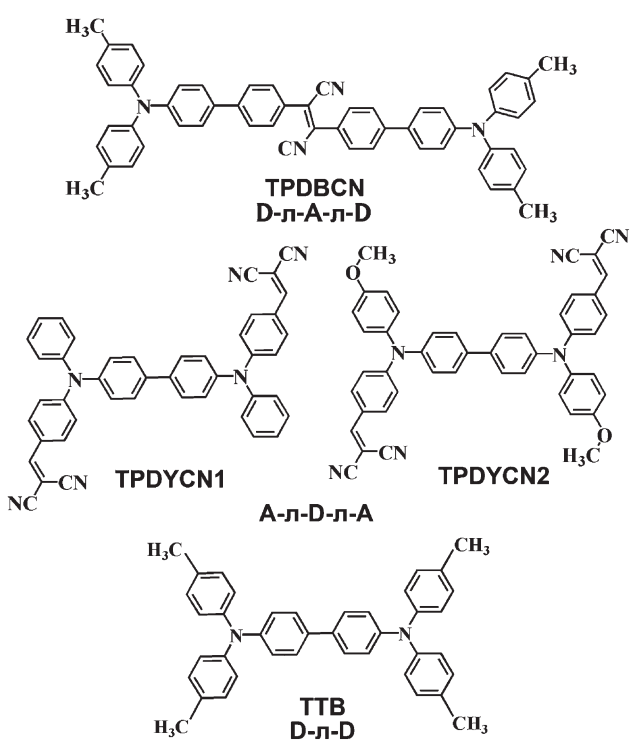

Figure 1. Molecular structures of TPDBCN, TPDYCN1, TPDYCN2, and TTB.

The thermal stability of the D–A molecules was studied by thermogravimetric analysis (TGA) in N_2. The temperatures for the onset of decomposition (T_d) of TPDBCN, TPDYCN1, and TPDYCN2 are about 235, 402, and 404 °C, respectively (Fig. S1, Supporting Information). This result indicates that the three D–A molecules have high thermal stability, which is very desirable for memory device stability.

The UV–vis absorption spectra of the three D–A molecules in dichloromethane solutions (10^{-5} M) and the thin films (30 nm on indium tin oxide—ITO) are shown in Figure S2 (Supporting Information). The absorption bands at around 470 nm can be assigned to the partial charge transfer (CT) between the donor and acceptor moieties of the D–A molecules,[31–34] which can also be proved by recording the absorption spectra of these compounds in a series of solvents with very different polarities (Fig. S3, Supporting Information). The CT transition in solid state shows an obvious red-shift compared with that of the solution state. This red-shift might be related to the formation of molecular head-to-tail aggregates and/or increased polarity of the thin film,[8,35,36] which would facilitate the occurrence of CT from the TPA to the acceptor moiety in neighboring molecules when an external electric field is applied.

2.2. Macroscopic Electrical Characterization

Memory devices of an ITO/organic layer/Al sandwich structure were fabricated using the three D–A molecules. The device structure is schematically shown in Figure 2a. The sweep directions and typical current–voltage (*I–V*) characteristics of the ITO/TPDBCN (30 nm thick)/Al device are shown in Figure 2b. When a forward voltage was applied, the thin film exhibited a low-conductance state (OFF state, curve I). As the voltage approached +1.4 V, a sharp increase in the current took place, indicating the thin film switched to a high-conductance state (ON state). After the transition, the thin film remained in the ON state during the second sweep from 0 to +1.7 V (curve II). This OFF–to–ON transition can be viewed in a memory device as a "writing" process. The ON state returned to the OFF state as the voltage approached −1.4 V when sweeping from 0 to −1.7 V (curve III). Then it showed an OFF state, as indicated by a followed reverse scan (curve IV). The OFF state could be switched back to the high-conductivity state by applying a positive bias higher than the threshold, resulting in an OFF–ON–OFF–ON reversible trait (Fig. S4a, Supporting Information). The maximum ON/OFF ratio was about 10^6, and that for all measured devices were typically greater than 10^4. Such a high ON/OFF current ratio is crucial for the memory device to realize high-resolution and low-error-rate data storage.[12,23,37] The results suggested that the memory device based on TPDBCN molecules exhibited excellent write–read–erase memory characteristics with a high ON/OFF ratio.

Figure 2c shows the typical *I–V* characteristics of an ITO/TPDYCN1 (30 nm thick)/Al device. As can be seen, there was an abrupt increase of the current in the device near +1.6 V when a positive voltage was applied (curve I). Once the device reached its ON state, it remained in this state, even after the power was turned off, or during sequential forward voltage sweeping (curve II) and reverse voltage sweeping (curve III, IV). The results indicated the

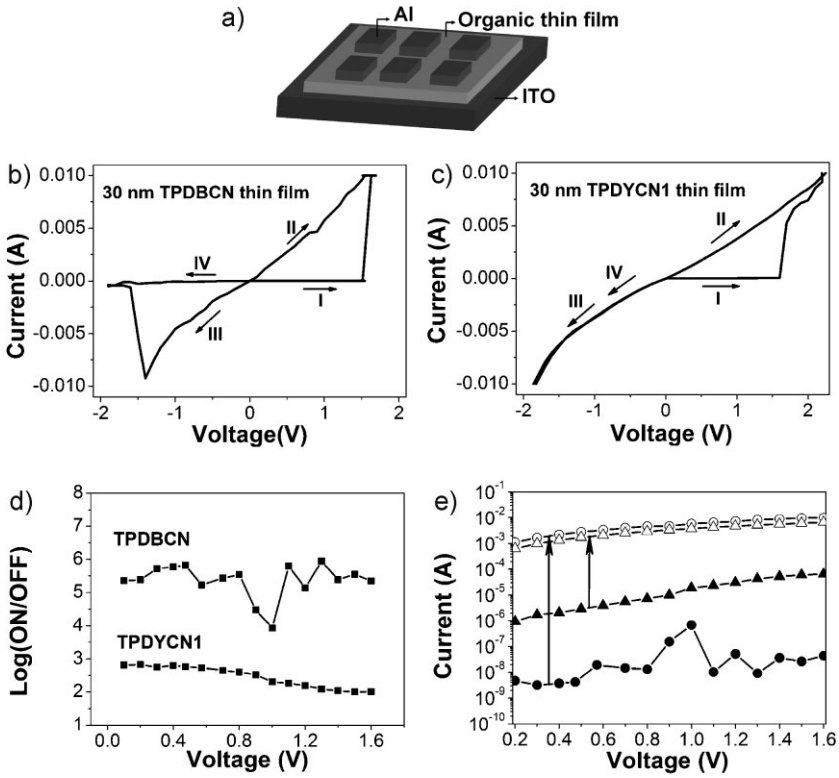

Figure 2. a) The device structure used for macroscopic *I–V* measurements. b) Macroscopic *I–V* characteristics of ITO/TPDBCN (30 nm thick)/Al. c) Macroscopic *I–V* characteristics of ITO/TPDYCN1 (30 nm thick)/Al. d) The comparison of the ON/OFF current ratio of b and c. e) The comparison of ON (open symbols) and OFF (filled symbols) state current in b (circles) and c (triangles); the arrows indicate transitions from OFF to ON state in each of the devices.

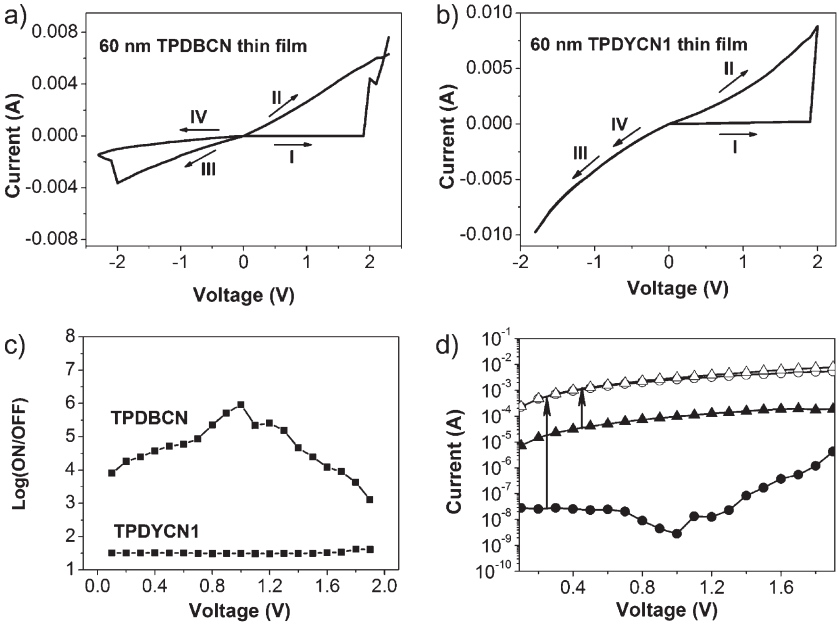

Figure 3. a) Macroscopic *I–V* characteristics of ITO/TPDBCN (60 nm thick)/Al. b) Macroscopic *I–V* characteristics of ITO/TPDYCN1 (60 nm thick)/Al. c) The comparison of the ON/OFF current ratios of a and b. d) The comparison of ON (open symbols) and OFF (filled symbols) state current in a (circles) and b (triangles); the arrows indicate transitions from OFF to ON state in each of the devices.

devices based on the TPDYCN1 molecules exhibited irreversible switching behavior. The ON/OFF current ratio was in the range of 10^2–10^3, which was relatively low compared with the device made by TPDBCN (Fig. 2d).

Then we compared the ON and OFF state current in the two devices (Fig. 2e). The data showed that both TPDBCN and TPDYCN1 devices had a high ON state current, while the OFF state current in the TPDBCN device was much lower than that of the TPDYCN1 device. Such results resulted in a high ON/OFF ratio between the current in the two states based on the TPDBCN device.

To extend the comparison of the electrical switching properties of the two molecules, we further varied the thickness of the organic layer and fabricated devices with 60 nm TPDBCN or TPDYCN1 thin films, and investigated their switching performance. As shown in Figure 3a–b, both devices exhibited similar behavior with that of their 30 nm thick films. That is, the 60 nm TPDBCN devices exhibited excellent write–read–erase memory characteristics with a high ON/OFF ratio of up to 10^6, while the TPDYCN1 devices exhibited irreversible switching behavior with a relatively low ON/OFF current ratio (Fig. 3c). The multiple *I–V* scans of the TPDBCN devices are shown in Figure S4b (Supporting Information). In the same way, the high ON/OFF ratio of 60 nm in the TPDBCN devices resulted from the relatively low OFF state current (Fig. 3d).

As known, electronic properties are highly dependent on the chemical structures and compositions of the materials. Although both the TPDBCN and TPDYCN1 molecules possessed the D–A conjugation backbone, the position of the acceptors in the molecules was rather different. In a D–л–A–л–D molecule, the acceptors reside at the middle; due to their electron-withdrawing nature,[12] they disturb the conjugation of the molecules. And quantum-tunneling probability through the molecule was decreased, resulting in very low OFF state current. After the conductance transition, the large conjugated tertiary amine system could stabilize the high-conductance state effectively, and resulted in a high ON state current. Thus, the high ON/OFF ratio was obtained in the TPDBCN devices. However, in an A–л–D–л–A molecule, the acceptors reside at the outer positions and hence do not perturb the conjugation as strongly as in the D–л–A–л–D molecule. The OFF state current is therefore higher; the ON/OFF ratio of a device based on A–л–D–л–A is hence low. Therefore, by controlling the arrangement of the acceptors and donors in the molecule, the ON/OFF ratio

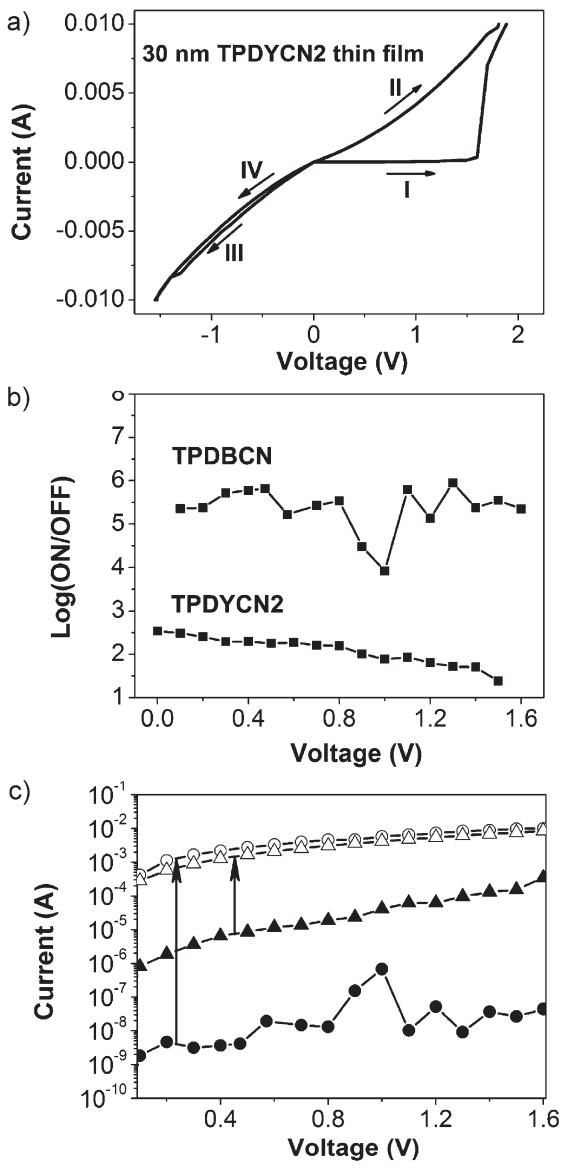

Figure 4. a) Macroscopic *I–V* characteristics of ITO/TPDYCN2 (30 nm thick)/Al. b) The comparison of ON/OFF current ratio in a and Fig. 2b. c) The comparison of ON (open symbols) and OFF (filled symbols) state current in a (triangles) and Fig. 2b (circles); the arrows indicate transitions from OFF to ON state in each of the devices.

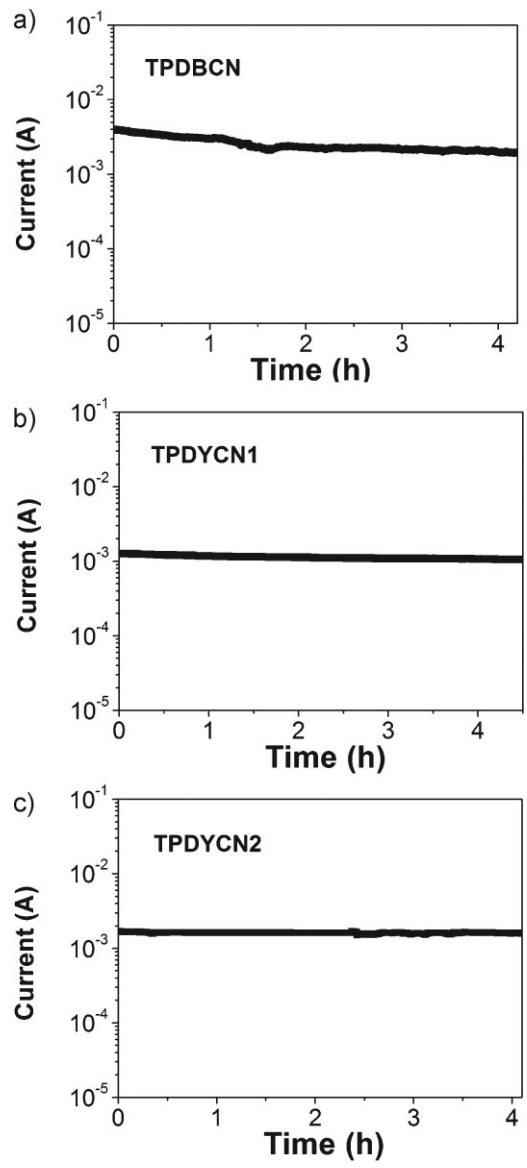

Figure 5. Long-term response of the ON state under an electric field of 0.5 V: a) TPDBCN, b) TPDYCN1, and c) TPDYCN2.

can be effectively improved, which is critical for designing high-performance switching materials.

In order to verify the results, another A–π–D–π–A style molecule, TPDYCN2, was synthesized, and the electrical switching behavior was investigated. As shown in Figure 4a, the ITO/TPDYCN2 (30 nm thick)/Al devices exhibit irreversible switching behavior that is similar to TPDYCN1 devices, with a write voltage of 1.6 V. Similarly, its relatively low ON/OFF ratio ((3.2×10^1)–(3.2×10^2)) resulted from its higher OFF state current compared with the TPDBCN devices (Fig. 4b,c). The results further indicated that the arrangement of the acceptors and donors in the backbone of the molecules play a key role for the ON/OFF ratio.

In addition to the ON/OFF current ratio, retention ability and threshold voltage are also important to the performance of a memory device. Thus the retention time of the ON state were also investigated. Thin films of the three D–A molecules were found to retain the ON state without obvious degradation under 0.5 V bias during more than 4 h of continuous operation (Fig. 5), which indicated the stability of the devices. Furthermore, it is worth emphasizing that the threshold voltages for both ON and OFF states are less than ±2 V for all of the devices, which might be attributed to the good charge-transporting ability of the triphenylamine units. The low operating voltage is desirable for low-power memory devices.[38,39]

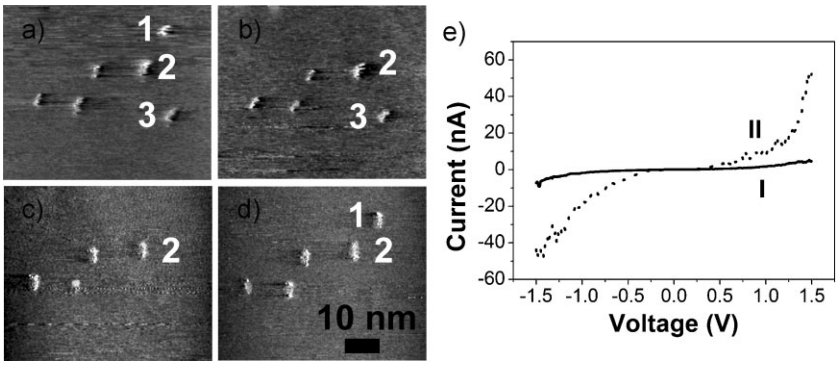

Figure 6. a) A typical STM image of the recorded pattern on the TPDBCN thin film: pulsed voltage, +2.46 V, 5 ms. b,c) Erasing one and two dots, respectively: pulsed voltage, −2.3 V, 5 ms. d) Rewriting one information dot: pulsed voltage, +2.46 V, 5 ms. e) Typical STM *I–V* curves in the unrecorded (curve I) and recorded region (curve II). STM was performed in constant-current mode with set points of bias voltage, $V_{bias} = 0.154$ V, and reference current, $I_{ref} = 0.131$ nA.

The nanoscale data storage was also achieved on TPDYCN1 and TPDYCN2 thin films by STM. Studies showed that when the applied voltage pulse was above the threshold (+2.7 V for TPDYCN1, and +3.0 V for TPDYCN2), the recorded dots could be easily formed. Figure 7a,c show the typical recording pattern on the TPDYCN1 and TPDYCN2 thin films; the average size of the recording marks was about 2.5 and 4 nm in diameter, respectively. The patterns were stable during the 8 h of continuous scanning. Scanning tunneling spectroscopy studies also indicated the applied voltage pulse induced a conversion of the conductance of the thin films from high to low resistance, which was in accordance with their macroscopic *I–V* characteristics, as shown in Figure 7b,d.

2.3. Nanoscale Data Storage and Local Electronic Properties

Based on the electrical bistability of the TPDBCN, TPDYCN1, and TPDYCN2 molecules, data recording experiments were performed with a P47 scanning tunneling microscope under ambient conditions using electrochemically etched tungsten tips. Thin films of each D–A molecule with a thickness of about 10 nm were deposited on the surface of a freshly cleaved highly oriented pyrolytic graphite (HOPG) substrate. To induce the recording dots, voltage pulses were applied between the STM tip and the HOPG substrate.

Figure 6a shows a typical STM image of the recorded pattern on the TPDBCN thin film. The recording dots with an average diameter of 4 nm were formed by applying program-controlled voltage pulses of +2.46 V and 5 ms. The pattern was stable during 8 h of scanning except for a slight thermal drift. Because of the reversible switching ability of the TPDBCN molecule, we further investigated the erase process of the recording dots. Further experiments indicated that when a reverse-polarity voltage pulse above 2.3 V was applied to the recorded region, the recorded marks could be substantially erased (Fig. 6b,c), and a new data mark can be rewritten on the erased region of the thin film by applying another positive pulsed voltage (Fig. 6d). With alternating electric field treatments of positive and negative voltages beyond the threshold value, write–read–erase cycles were demonstrated in the same area. The local *I–V* characteristics of the TPDBCN thin film were compared between the recorded and unrecorded regions to obtain insights into the mechanism for the formation of the information dots. As can be seen in Figure 6e, the conductivity of unrecorded regions on the film was in a high resistance state (curve I), while it was in a low resistance state at the recorded regions (curve II). The reproducibility of the local *I–V* curves is shown in Figure S4c (Supporting Information). The comparisons presented herein indicate that the applied voltage pulse induced a conversion of the conductance of the thin film from a high resistance to a low one, which was in accordance with the macroscopic *I–V* characteristics.

2.4. Mechanism Discussion

The conductance transitions based on organic materials have been rationalized using different mechanisms.[1] A field-induced charge transfer is generally regarded as the main reason for the switching behavior in a D–A system.[26,27] To understand the electrical switching behavior of the D–A molecules in this work, a D–л–D structural molecule (TTB) composed of only two TPA units without any acceptor was studied for comparison. Macroscopic *I–V* characteristics showed that the conductance transition occurred neither in forward nor backward sweeping for the ITO/TTB

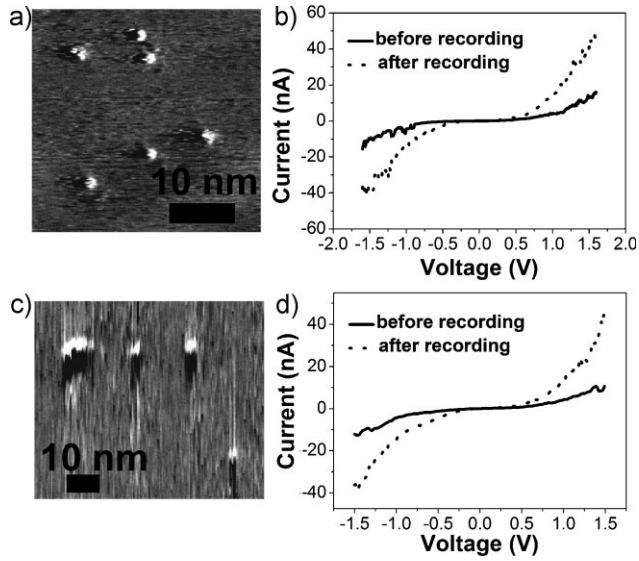

Figure 7. STM images of typical information dots pattern and the corresponding *I–V* curves on the thin films of a,b) TPDYCN1: pulsed voltage, +2.73 V, 5 ms. Tunneling conditions: $V_{bias} = 0.154$ V, $I_{ref} = 0.131$ nA. c,d) TPDYCN2: pulsed voltage, +3 V, 3 ms. Tunneling conditions: $V_{bias} = 0.154$ V, $I_{ref} = 0.131$ nA.

(30 nm thick)/Al device (Fig. S5, Supporting Information). This result indicates the electrical switching behavior could not occur in the D–π–D structure, and that the D–A structure is vital for the electrical switching of the memory device. Thus charge transfer, mediated by the arrangement of the donor and acceptor located in the molecular backbone, is probably responsible for the conductance switching and the associated memory behavior.

In order to further understand the electrical switching behavior, quantum chemical calculations were performed using the hybrid Hartree–Fock/density functional theory (HF/DFT) method of B3LYP with the 6-31G* basis set.[40] The highest occupied molecular orbital (HOMO) and the lowest unoccupied molecular orbital (LUMO) surfaces for the three molecules are shown in Figure 8. The HOMO and LUMO surfaces obtained were unevenly distributed, with the former preferring to localize on the electron donor side and the latter on the electron acceptor side. The HOMO–LUMO gap was 2.28, 2.95, and 2.86 eV for TPDBCN, TPDYCN1, and TPDYCN2, respectively. The results indicated that the HOMO of the molecule might interact with the LUMO for charge transfer. Generally, charge transfer includes both intramolecular and intermolecular charge transfer. They are competitive and can coexist in a single molecular material.[41,42] In this case, the molecules tend to adopt an offset head-to-tail packing mode in the thin film as revealed by Figure S2 (Supporting Information). The packing mode would facilitate the occurrence of intermolecular charge transfer from the electron donor to the acceptor when an external electric field has been exerted.

When the terminal moieties of the molecule were electron donors and the central moieties were electron acceptors such as the TPDBCN molecule, it was obvious that the π-conjugated system throughout the molecule was perturbed by acceptors owing to their electron-withdrawing nature. This conclusion is further supported by comparative calculations on a structure where the cyano groups (with strong electron-withdrawing nature) have been replaced by groups of similar steric bulk, but of different electron demand, e.g., methyl groups, which are slightly electron-releasing (Fig. S6, Supporting Information). The localization of the electron density of TPDBCN in the HOMO resulted in very low OFF state current. When the right voltage pulse was exerted on the thin film, charge was transferred from the donor of one molecule to the acceptor of the neighboring molecule, resulting in an increased number of carriers and a delocalized state, and the conductance of the system is increased.[26] In the meantime, TPA, as a large conjugated tertiary amine system, cannot only act as a strong electron donor in its neutral state, but also as a stabilizer to the delocalized state, thus the higher conductivity can be maintained.[5] Under a reversed bias, acceptor groups lost the charge state to neutralize the positively charged TPA moieties, and the thin film returned to low conductance state.

However, when the acceptors were located in the terminal of the molecules as TPDYCN1 and TPDYCN2, they had little influence on the conjugation of the backbone. The electron density in the HOMO was delocalized throughout the whole molecule, thus resulting in a relatively high OFF state current. On the other hand, the differences in the structural symmetry played an important factor in governing the recording reversibility. TPDYCN1 and TPDYCN2 molecules had bent structures that resulted in larger dipole moments than TPDBCN which possessed a linear structure (Fig. 8). Upon HOMO to LUMO transition, a much larger dipole moment would be formed for the excited state because of the considerable increase in charge separation.[8] Meanwhile, because the flexible C−C single bond between the two TPA units could acquire a higher degree of conformational freedom by charge transfer interaction, they were able to undergo reorientation and resulted in the change of the initial molecular conformation. Such conformational changes might favor the charge separation, which would also enhance the polarity of the molecule.[43,44] Consequently, both the charge transfer and conformational change could greatly facilitate the stability of the charge-separated state because of the formation of the strong

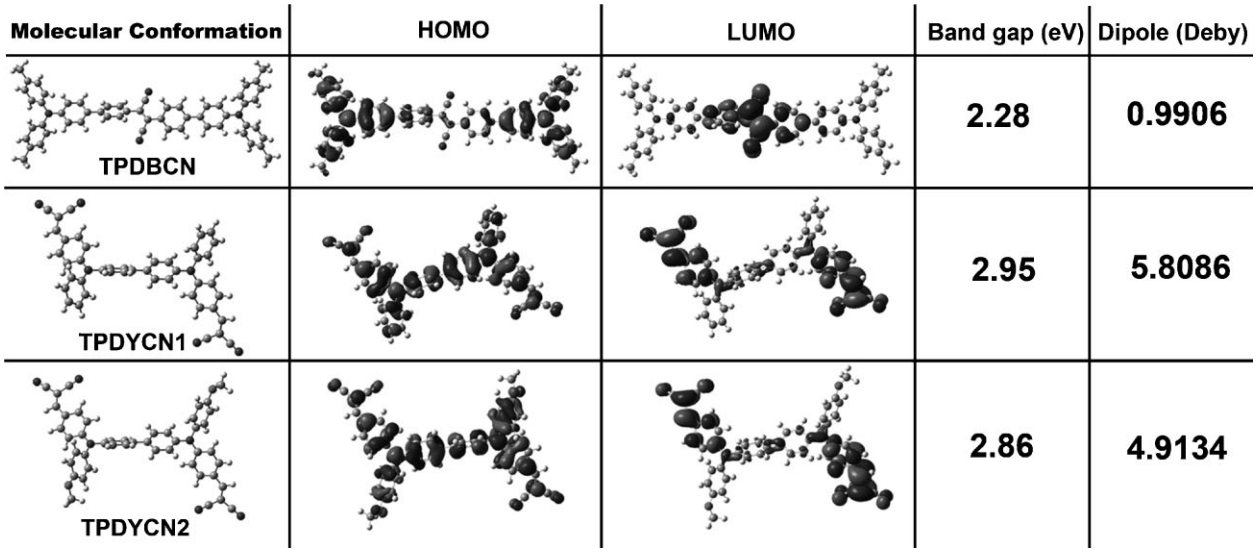

Figure 8. The molecular conformation, HOMO and LUMO molecular orbitals, bandgap and dipole of a) TPDBCN, b) TPDYCN1, and c) TPDYCN2 calculated by the HF/DFT method of B3LYP with the 6-31G* basis set.

dipole moment, thus irreversible switching behavior was observed even after the application of a reverse polarity bias.

3. Conclusions

In this work, we illustrated the effect of the arrangement of triphenylamine-based D–A molecules on the electric field-induced switching properties. The devices based on the D–л–A–л–D molecule exhibited excellent write–read–erase characteristics with a high ON/OFF ratio of 10^4–10^6. While the devices based on the A–л–D–л–A molecules exhibited irreversible switching behavior with an ON/OFF ratio of about (3.2×10^1)–(1×10^3). Moreover, long retention time of the high conductance state and low threshold voltage were observed for the D–A molecules owing to the large conjugated tertiary amine system and good hole-transporting ability of the triphenylamine units. Accordingly, stable and reliable nanoscale data storage was achieved on the thin films of the three D–A molecules by STM. The results will be of great significance for guiding the design of new molecular systems to improve the electronic switching properties (ON/OFF current ratio, reversibility, etc.) and to achieve high-performance data storage.

4. Experimental

Materials: TTB is commercially available. TPDBCN, TPDYCN1 and TPDYCN2 were prepared in our laboratory, and their structures were confirmed by ^{1}H NMR ($CDCl_3$, 400 MHz), ^{13}C NMR ($CDCl_3$, 100 MHz), matrix-assisted laser desorption/ionization time-of-flight mass spectrometry (MALDI-TOF MS; m/z), and elemental analysis. All of the materials were purified by vacuum sublimation before use.

Fabrication of the Memory Devices and Experimental Information: The ITO substrate was precleaned sequentially with water, ethanol, and acetone in an ultrasonic bath for 20 min. By physical vacuum vapor deposition method, the organic thin films for macroscopic *I–V* measurements were deposited onto ITO. The organic molecules were heated in a crucible, and the base vacuum of the deposition system was about 4.5×10^{-4} Pa, and deposition rate was controlled about 0.3–0.7 Å s^{-1}. The thermal vapor temperatures of TPDBCN, TPDYCN1, TPDYCN2, and TTB were 180, 150, 140, and 95 °C, respectively. Al top electrodes of about 150 nm in thickness were finally deposited on the organic thin films surface through a shadow mask. Active device area of 1 mm × 2.5 mm was obtained. The macroscopic *I–V* characteristics were obtained by scanning the voltage using a Keithley 4200 semiconductor system. The amplitude of applied voltage was varied to generate a range of *I–V* characteristics, and the voltages were changed in steps of 0.1 V. All electrical experiments were conducted in ambient air.

The thin films for the data storage experiment with STM were thermally evaporated and deposited on freshly cleaved HOPG substrate. STM (Solver P47 instrument, NT-MDT Co.) images were recorded in constant current mode in ambient atmosphere at room temperature. The bias voltage was applied to the substrate. The data recording/erasing experiment was performed by a program-controlled STM tip. Electrochemically etched tungsten tips were used for both STM and scanning tunneling spectroscopy (STS) studies. The recording experiments were carried out by applying voltage pulses between the tungsten tip and HOPG substrate, and STS was used to probe the local electronic properties of the thin films. When voltage pulses were added, the feedback loop was closed and the STM tip was lifted up a short distance from the tunneling position to avoid running into the thin film surface.

The UV–vis spectra were recorded on a Hitachi U4100 spectrophotometer. TGA was conducted on an EXSTAR6000 TG/DTA6300 analyzer at a heating rate of 10 °C min^{-1} and under an N_2 flow.

Acknowledgements

This work was supported by the NSFC (Grant Nos. 50625312, 60601027, 20421101, U0634004), 973 Program (No. 2006CB806200, 2006CB932100, 2006CB921706, 2007CB936403 and 2009CB930404) and Chinese Academy of Sciences. Supporting Information is available online from Wiley Interscience or from the authors.

Received: September 8, 2009
Revised: October 19, 2009
Published online: February 9, 2010

[1] J. C. Scott, L. D. Bozano, *Adv. Mater.* **2007**, *19*, 1452.
[2] G. Y. Jiang, Y. L. Song, X. F. Guo, D. Q. Zhang, D. B. Zhu, *Adv. Mater.* **2008**, *20*, 2888.
[3] T. J. Lee, S. Park, S. G. Hahm, D. M. Kim, K. Kim, J. Kim, W. Kwon, Y. Kim, T. Chang, M. Ree, *J. Phys. Chem. C* **2009**, *113*, 3855.
[4] G. Liu, Q.-D. Ling, E. Y. H. Teo, C.-X. Zhu, D. S.-H. Chan, K.-G. Neoh, E.-T. Kang, *ACS Nano* **2009**, *3*, 1929.
[5] Q.-D. Ling, F.-C. Chang, Y. Song, C.-X. Zhu, D.-J. Liaw, D. S.-H. Chan, E.-T. Kang, K.-G. Neoh, *J. Am. Chem. Soc.* **2006**, *128*, 8732.
[6] Y. L. Liu, K. L. Wang, G. S. Huang, C. X. Zhu, E. S. Tok, K. G. Neoh, E. T. Kang, *Chem. Mater.* **2009**, *21*, 3391.
[7] L. H. Xie, Q. D. Ling, X. Y. Hou, W. Huang, *J. Am. Chem. Soc.* **2008**, *130*, 2120.
[8] S. L. Lim, N.-J. Li, J.-M. Lu, Q.-D. Ling, C. X. Zhu, E.-T. Kang, K. G. Neoh, *ACS Appl. Mater. Interfaces* **2009**, *1*, 60.
[9] S. Choi, S. H. Hong, S. H. Cho, S. Park, S. M. Park, O. Kim, M. Ree, *Adv. Mater.* **2008**, *20*, 1766.
[10] Z. J. Donhauser, B. A. Mantooth, K. F. Kelly, L. A. Bumm, J. D. Monnell, J. J. Stapleton, D. W. Price, A. M. Rawlett, D. L. Allara, J. M. Tour, P. S. Weiss, *Science* **2001**, *292*, 2303.
[11] C. P. Collier, G. Mattersteig, E. W. Wong, Y. Luo, K. Beverly, J. Sampaio, F. M. Raymo, J. F. Stoddart, J. R. Heath, *Science* **2000**, *289*, 1172.
[12] A. Bandhopadhyay, A. J. Pal, *J. Phys. Chem. B* **2003**, *107*, 2531.
[13] S. Sahu, A. J. Pal, *Org. Electron.* **2008**, *9*, 873.
[14] C. Pearson, J. H. Ahn, M. F. Mabrook, D. A. Zeze, M. C. Petty, K. T. Kamtekar, C. Wang, M. R. Bryce, P. Dimitrakis, D. Tsoukalas, *Appl. Phys. Lett.* **2007**, *91*, 123506.
[15] C.-H. Tu, Y.-S. Lai, D.-L. Kwong, *Appl. Phys. Lett.* **2006**, *89*, 062105.
[16] T. Tsujioka, H. Kondo, *Appl. Phys. Lett.* **2003**, *83*, 937.
[17] M. Feng, L. Gao, Z. Deng, W. Ji, X. Guo, S. Du, D. Shi, D. Zhang, D. Zhu, H. Gao, *J. Am. Chem. Soc.* **2007**, *129*, 2204.
[18] H. J. Gao, K. Sohlberg, Z. Q. Xue, H. Y. Chen, S. M. Hou, L. P. Ma, X. W. Fang, S. J. Pang, S. J. Pennycook, *Phys. Rev. Lett.* **2000**, *84*, 1780.
[19] L. P. Ma, Y. L. Song, H. J. Gao, W. B. Zhao, H. Y. Chen, Z. Q. Xue, S. J. Pang, *Appl. Phys. Lett.* **1996**, *69*, 3752.
[20] H. Tian, Q. C. Wang, *Chem. Soc. Rev.* **2006**, *35*, 361.
[21] J. Y. Ouyang, C. W. Chu, C. R. Szmanda, L. P. Ma, Y. Yang, *Nat. Mater.* **2004**, *3*, 918.
[22] L. Ma, J. Liu, S. Pyo, Y. Yang, *Appl. Phys. Lett.* **2002**, *80*, 362.
[23] Q. Lai, Z. Zhu, Y. Chen, S. Patil, F. Wudl, *Appl. Phys. Lett.* **2006**, *88*, 133515.
[24] M. Ouyang, S. M. Hou, H. F. Chen, K. Z. Wang, *Phys. Lett. A* **1997**, *235*, 413.
[25] B. Mukherjee, A. J. Pal, *Chem. Mater.* **2007**, *19*, 1382.
[26] Y. L. Shang, Y. Q. Wen, S. L. Li, S. X. Du, X. B. He, L. Cai, Y. F. Li, L. M. Yang, H. J. Gao, Y. Song, *J. Am. Chem. Soc.* **2007**, *129*, 11674.
[27] L. P. Ma, W. J. Yang, Z. Q. Xue, S. J. Pang, *Appl. Phys. Lett.* **1998**, *73*, 850.
[28] N. von Malm, J. Steiger, R. Schmechel, H. von Seggern, *J. Appl. Phys.* **2001**, *89*, 5559.
[29] S. Tokito, Y. Taga, *Mol. Cryst. Liq. Cryst.* **2000**, *349*, 389.

[30] P. J. Low, M. A. J. Paterson, A. E. Goeta, D. S. Yufit, J. A. K. Howard, J. C. Cherryman, D. R. Tackley, B. Brown, *J. Mater. Chem.* **2004**, *14*, 2516.
[31] S. Roquet, A. Cravino, P. Leriche, O. Aleveque, P. Frere, J. Roncali, *J. Am. Chem. Soc.* **2006**, *128*, 3459.
[32] A. P. Kulkarni, X. X. Kong, S. A. Jenekhe, *Adv. Funct. Mater.* **2006**, *16*, 1057.
[33] P. F. Xia, X. J. Feng, J. P. Lu, S. W. Tsang, R. Movileanu, Y. Tao, M. S. Wong, *Adv. Mater.* **2008**, *20*, 4810.
[34] S. J. Lo, W. S. Li, Y. H. Chen, I. Chao, *Chem. Eur. J.* **2005**, *11*, 6533.
[35] M. Surin, P. Sonar, A. C. Grimsdale, K. Mullen, S. De Feyter, S. Habuchi, S. Sarzi, E. Braeken, A. V. Heyen, M. Van der Auweraer, F. C. De Schryver, M. Cavallini, J. F. Moulin, F. Biscarini, C. Femoni, L. Roberto, P. Leclere, *J. Mater. Chem.* **2007**, *17*, 728.
[36] L. Zhang, Y. Zhang, H. B. Tao, X. J. Sun, Z. J. Guo, L. G. Zhu, *Thin Solid Films* **2002**, *413*, 224.
[37] Q.-D. Ling, S.-L. Lim, Y. Song, C.-X. Zhu, D. S.-H. Chan, E.-T. Kang, K.-G. Neoh, *Langmuir* **2007**, *23*, 312.
[38] T. L. Choi, K. H. Lee, W. J. Joo, S. Lee, T. W. Lee, M. Y. Chae, *J. Am. Chem. Soc.* **2007**, *129*, 9842.
[39] S. G. Hahm, S. Choi, S. H. Hong, T. J. Lee, S. Park, D. M. Kim, W. S. Kwon, K. Kim, O. Kim, M. Ree, *Adv. Funct. Mater.* **2008**, *18*, 3276.
[40] C. T. Lee, W. T. Yang, R. G. Parr, *Phys. Rev. B* **1988**, *37*, 785.
[41] M. Knupfer, T. Schwieger, H. Peisert, J. Fink, *Phys. Rev. B* **2004**, *69*, 165210.
[42] M. Zheng, F. L. Bai, D. B. Zhu, *Polym. Adv. Technol.* **2003**, *14*, 292.
[43] Z. R. Grabowski, K. Rotkiewicz, W. Rettig, *Chem. Rev.* **2003**, *103*, 3899.
[44] G. Y. Jiang, Y. L. Song, Y. Q. Wen, W. F. Yuan, H. M. Wu, Z. Yang, A. D. Xia, M. Feng, S. X. Du, H. J. Gao, L. Jiang, D. B. Zhu, *ChemPhysChem* **2005**, *6*, 1478.